

Spatial and Spectral Resolution Considerations for Imaging Coastal Waters

Curtiss O. Davis^a, Maria Kavanaugh^a, Ricardo Letelier^a, W. Paul Bissett^b and David Kohler^b
^aCollege of Oceanic and Atmospheric Sciences, Oregon State University, Corvallis, OR 97331,
USA

^bFlorida Environmental Research Institute Tampa, FL, 33612, USA

ABSTRACT

Current ocean color sensors, for example SeaWiFS and MODIS, are well suited for sampling the open ocean. However, coastal environments are spatially and optically more complex and require more frequent sampling and higher spatial resolution sensors with additional spectral channels. We have conducted experiments with data from Hyperion and airborne hyperspectral imagers to evaluate these needs for a variety of coastal environments. Here we present results from an analysis of airborne hyperspectral data for a Harmful Algal Bloom in Monterey Bay. Based on these results and earlier studies we recommend increased frequency of sampling, increased spatial sampling and additional spectral channels for ocean color sensors for coastal environments.

Keywords: coastal, ocean, hyperspectral, remote sensing, ocean color

1 INTRODUCTION

Current ocean color sensors, for example SeaWiFS¹ and MODIS² and in the future VIIRS³, are well suited for sampling the open ocean. However, coastal environments are spatially and optically more complex and require more frequent sampling and higher spatial resolution sensors with additional spectral channels. To address those issues NOAA had considered including a hyperspectral Coastal Waters imaging capability (HES-CW) as part of the Hyperspectral Environment Suite (HES) on the next generation Geostationary Operational Environmental Satellite (GOES-R). The key advantage of a geostationary imager is frequency of revisit. Coastal waters are highly dynamic. Tides, diurnal winds, river runoff, upwelling and storm winds drive currents from one to several knots. Three hour or better sampling is required to resolve these features, and to track red tides, oil spills or other features of concern for coastal environmental management. To prepare for the possibility of HES-CW NOAA formed the Coastal Ocean Applications and Science Team (COAST)⁴. In September 2006 COAST conducted an experiment in Monterey Bay using airborne hyperspectral data to evaluate the need for higher frequency and higher spatial and spectral resolution sampling for the coastal ocean. Subsequent to that experiment NOAA has dropped HES from GOES-R. NOAA still recognizes that it has strong requirements for a coastal waters imager, but it has no specific plan at this time to meet those requirements.

Here we use data from the COAST Monterey Bay experiment to address the issues of frequency and spatial and spectral sampling for the coastal ocean. We present results from those analyses and recommend sampling frequency and spatial sampling resolution and spectral channels for ocean color sensors designed for coastal environments. Compared to polar orbiting ocean color sensors, such as MODIS and VIIRS, a Coastal Waters Imaging System (for convenience we call it CWIS though there is no specific instrument that meets these requirements at this time) should have significantly improved temporal, spatial and spectral sampling that will greatly enhance our ability to monitor and assess the dynamics of the coastal ocean. The following sections discuss the advantages of these key improvements.

1.1 The Case for Higher Frequency Temporal Sampling in Coastal Waters

The addition of a capability to view coastal waters several times a day either from a geostationary platform or with multiple satellites in low earth orbit will provide the management and science community with a unique capability to observe the dynamic coastal ocean environment. Tides (Fig. 1), diurnal winds (such as the land/sea breeze), river runoff,

upwelling and storm winds drive coastal currents that can reach several knots. Furthermore, currents driven by diurnal and semi-diurnal tides reverse approximately every 6 hours. A minimum sampling frequency of three hours is required to resolve these features, and to track water masses containing Harmful Algal Blooms (HABs), oil spills or other features of concern for coastal environmental management that are driven by these currents. Sampling once per day, as is currently planned for VIIRS will not adequately sample these dynamics.

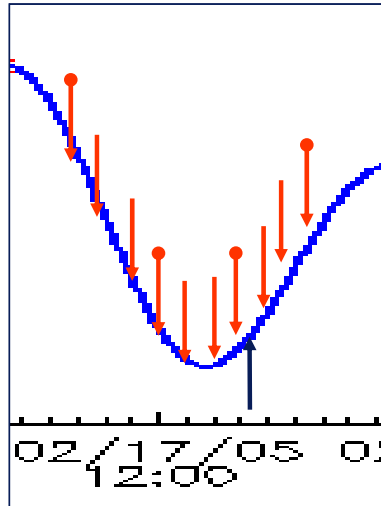


Fig. 1. Example tidal cycle from Charleston, OR. The tidal range is more than 4 m and tidal currents on the Oregon coast can exceed 2 knots. Black arrow VIIRS sampling at 1:30 PM local time; red arrows show hourly CWIS sampling. Red arrows with dots are once every three hours, which is the minimum sampling frequency needed to resolve a tidal cycle.

Federal and state agencies are responsible for the management of fisheries, monitoring of water quality, protection of marine sanctuaries and marine mammal habitats, assessing the effects of storm events and other issues related to the use and protection of the coastal ocean. Each of these management responsibilities requires an improved understanding of coastal ocean dynamics. Considerable progress has been made in our ability to monitor ocean color and temperature in the open ocean using the polar-orbiting satellites. However, the present once-a-day coverage from polar-orbiting satellites, which is further limited by clouds, is not sufficient to sample the dynamics of the coastal ocean. A CWIS would improve our ability to obtain usable imagery several times a day to resolve, among others, the effects of tides and wind events on coastal currents, and to understand changes in coastal water features that occur over a daily cycle. This capability will greatly improve our ability to manage coastal resources just as GOES imagery has improved our ability to monitor and forecast the weather.

Ocean color imaging requires sunlight and cloud free scenes. One advantage of geostationary imaging is the ability to wait until an area is cloud free, rather than sampling at one fixed time as set by the orbit for current polar orbiting ocean color imagers like SeaWiFS and MODIS. The capability to obtain frequent cloud-free imagery will be an important asset to water quality monitoring because surface currents can alter phytoplankton and sediment distributions near the coast and because phytoplankton growth rates which can exceed a doubling per day can rapidly alter water quality. Monitoring of water quality parameters from satellite, particularly from coastal regions susceptible to harmful algal blooms, is improved by the capability to access imagery on any given day. The frequent image acquisition available from a geostationary satellite or multiple low-earth satellites will improve the chances of obtaining a cloud-free image and allow imagery collected at different times of the day in various sub regions to be combined to generate daily cloud-free coastal ocean color scenes for the entire region.

We begin our study of the temporal requirements for CWIS using airborne hyperspectral data that was collected as frequently as once every half hour during the COAST Monterey Bay experiment (see below). This data will be ideal to address the issue of frequency of sampling. Initial results are presented in this paper, with guidance for future work.

1.2 The Case for Improved Spatial Sampling in Coastal Waters

The U. S. coastline is very complex with many sounds, bays and estuaries. In terms of area coverage the 300 m spatial resolution recommended for a CWIS is approximately 10 times better than the approximately 1000 m resolution currently available from polar orbiting ocean color imagers (90,000 m² per pixel compared to 1,000,000 m²). This higher spatial resolution will greatly enhance the ability to image and monitor complex areas like Chesapeake Bay, Puget Sound and the Florida Keys. For example (Fig. 2) the higher resolution will make it possible to image the Potomac River and other rivers feeding into the Chesapeake Bay that are missed at one kilometer resolution.

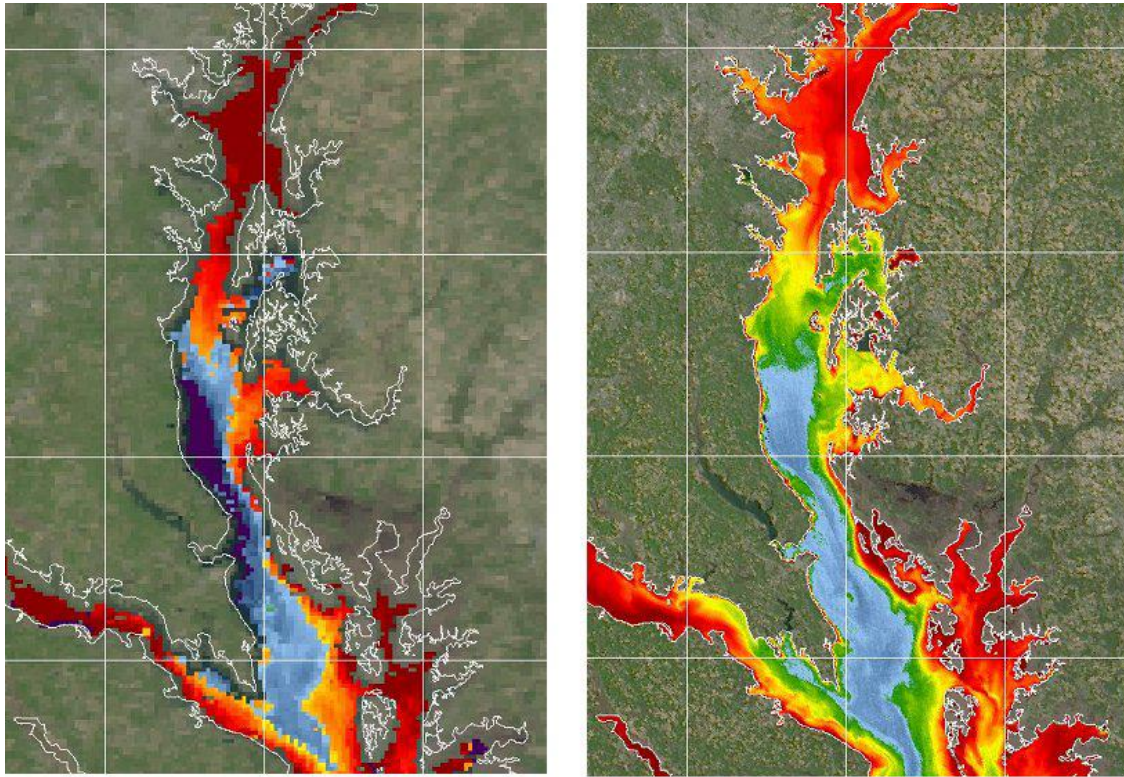


Fig. 2. Left, MODIS 1 km resolution image of water clarity for the Chesapeake Bay and the Potomac River (lower left corner of image) as it feeds into Chesapeake Bay. Right, 250 m resolution water clarity image simulated from the MODIS 1 km ocean color channels and the 250 m land channels. The land water interface is shown in white.

Outside of the bays and estuaries, the greatest impacts of HABs, as well as other features of interest in the near coastal ocean, such as sea grass beds and coral reefs, require a higher sampling in the spatial domain to resolve unique features of interest. Pixel contamination by land reflectance and the inability to separate unique features are just a couple of the problems that are seen in the data from low spatial resolution ocean color sensors. A previous study to determine the optimal Ground Sample Distance (GSD) for turbid coastal waters suggest that variance in near shore color requires a GSD of < 100 m to resolve the changes in high resolution reflectance measurements⁵. In addition, many of the ocean color algorithms rely on non-linear equations to retrieve Environmental Data Records (EDRs). In the coastal zone, where significant changes in optical and ecological properties occur on the scales of meters, the blending of the reflectance signal may result in EDRs that are not representative of the actual condition environmental conditions. In this study we address the spatial resolution necessary to image a HAB in Monterey Bay. We also discuss the spatial sampling requirements for sampling the bottom based on earlier work with Hyperion images of Florida Bay and the Keys.

1.3 The Case for Increased Spectral Sampling in Coastal Waters

Experience with airborne systems and Hyperion on NASA's EO-1 spacecraft^{5,6} has shown that the continuous spectra obtained with a hyperspectral instrument can greatly improve our ability to resolve the complexity of the coastal ocean. Having the full spectral data is particularly important when imaging the bottom⁷. Here we address the ability to address an important coastal ocean problem (i.e. HAB) with airborne hyperspectral data, with analysis of the data at continuous 14 nm spectral resolution and at the simulated multispectral resolution of MODIS and MERIS⁸ channels.

2 DATA AND METHODS

2.1 Monterey Bay Experiment, September 3-15, 2006

The first COAST experiment was conducted in Monterey Bay September 3-15, 2006. There are no existing data sets that include all the key attributes of geostationary ocean color data. The goal of this experiment was to collect data that exceeds all possible requirements for a geostationary ocean color imager so that the data may be binned spatially or spectrally to create a simulated data set for any possible set of requirements. For the Monterey Bay experiment we used the Florida Environmental Research Institute's (FERI) Spectroscopic Aerial Mapper with On-board Navigation (SAMSON; Fig. 3). SAMSON collects a full hyperspectral dataset covering 256 bands in the VNIR (3.5 nm resolution over 380 to 970 nm range) at 75 frames per second. It is designed with a Signal-to-Noise Ratio (SNR), stability, dynamic range, and calibration sufficient for dark target spectroscopy. Monterey Bay was sampled at 5 m Ground Sample Distance (GSD) and for this study we binned the data by 2 spatially and 4 spectrally to give 10 m GSD, 14 nm spectral data as the base data set. Flight logs from this experiment may be found at <http://www.feriweb.org/data/flightlogs/#GOESR>. Additional spectral and spatial binning was performed as a part of the analysis performed in this study as described in section 2.2 below.



Fig. 3. The Spectroscopic Aerial Mapper with On-board Navigation (SAMSON). The hyperspectral imager is black object in the foreground. The black box at the top of the image is the integrated inertial navigation system which sits atop a high resolution framing camera. The yellow frame is the motion compensation mounting system.

Two ships the R/V John H. Martin and the R/V Shana Rae were used during the experiment. A wide range of *in situ* measurements were made on the ships including:

absorption scattering, a_{cdom} (a_{c9} , a_{cs})
 Backscattering (Hydroscat and Puck)
 CDOM (fluorescence, waveguide)
 CHL fluorescence
 Remote sensing reflectance (above, in-water)
 Diffuse attenuation coefficient – $k(490,532)$
 $Lu(+)$. Radiance, $ED+$ irradiance (HTSRB)
 PAR (downwelling)
 Volume Scattering Function (ECO-VSF)
 Radiance distribution – (NURADS)
 Particle Size (LISST) (forward scattering) (green)
 PC02 (underway)
 Phytoplankton communities (underway)
 Conductivity, temperature and Depth (CTD)
 Aerosol optical depth –Microtops

At selected depths water samples were collected and returned to the laboratory for additional measurements:

$a_{(detrital)}$ filterpad absorption
 $a_{(cdom)}$ (filterpad absorption)
 POM Particulate - organic
 PIM Particulate - inorganic
 SPM Suspended
 HPLC (pigments)
 CHL (Fluorescence)
 Nutrients
 Primary Production
 Fluorescence
 PC02
 Phytoplankton communities

This data is used to characterize the in-water conditions at the time of each overflight including the HAB seen in Monterey Bay during the experiment. The *in situ* data is not presented in this paper, but it is used to interpret the in water features seen in the SAMSON images described in this paper.

Earlier measurements identified a HAB in the northeast corner of Monterey Bay. Because of the interest in monitoring such blooms the experiment was focused in that part of the Bay. SAMSON was flown on grid covering that region that could be completed in 30 minutes. The grid was repeated for up to 5 hours to simulate the time series of data that could be acquired from a geostationary ocean color imager. The data was calibrated⁹, and ortho-rectified overnight to provide an initial product that was viewed the next day by the research team to plan the following day's experiments. Analysis of the spectra showed a prominent spectral peak at 709 nm that was indicative of the HAB. Fig. 4 shows a map of the northeast corner of Monterey Bay using the 709 nm channel as an indicator of the HAB. We noted rapid changes in the depth and location of the HAB in sequential images. For this study we selected a square region (the box in Fig. 4) that was sampled in every image to look at the changes with time during one day (September 12, 2006) and between days (September 12th and 15th).

All of the data was processed to an initial level during the experiment. Final reprocessing of the SAMSON and *in situ* data is underway and all of the results will be available on WEOGEO a web-based server at the Florida Environmental Research Institute (FERI) with a duplicate server at OSU (<http://weogeo.coas.oregonstate.edu>).

During the experiment mid-summer foggy conditions persisted until the last day of the experiment limiting remote sensing opportunities. In spite of that we collected SAMSON Airborne hyperspectral data on Sept 5, 11, 12, and 15. Ship data was collected on those dates and additional measurements were made on cloudy days. Mooring and glider data were collected throughout the experiment. Overall we collected an exceptional data set for characterization of the HAB biology, optics and remote sensing characteristics. On the last day of the experiment (September 15th) a dry cold front passed through the area thoroughly disrupting the HAB; this dramatic change is documented in the remote sensing and *in situ* data.

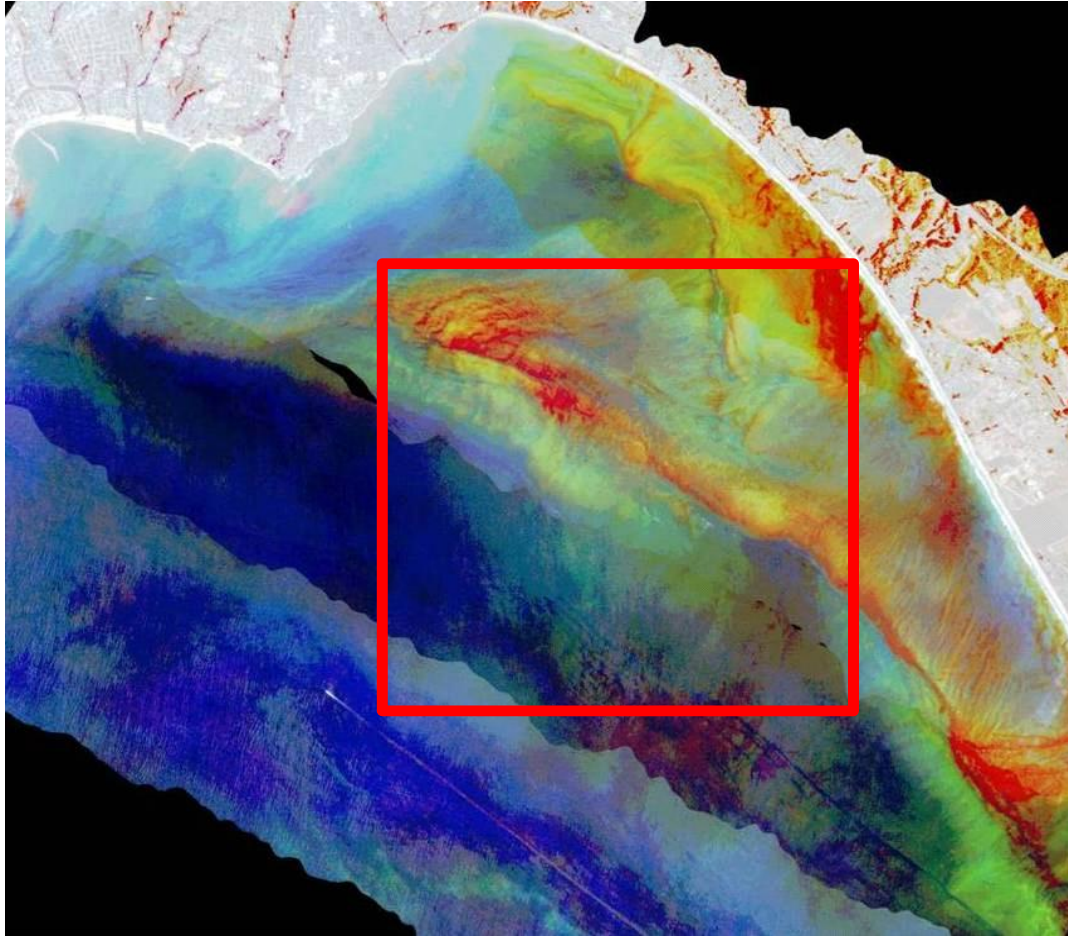


Fig. 4. SAMSON image of the northeast corner of Monterey Bay. This is the third map collected on September 12, 2006. Four flight lines are shown that have been geolocated to one pixel accuracy and mosaiced to produce the image. The surface HAB is identified using the 709 nm band and is indicated in red in the image. The adjacent regions in yellow also have high levels of phytoplankton. The bloom is a mix of species, but predominately the dinoflagellate *Akashiwo sanguinea*. The box indicates the subset of the image used in the analyses reported in this paper.

2.2 Data Analysis Methods

Here we report an analysis of several images of the northeast corner of Monterey Bay off the coast of central California in order to determine (i) the dominant scales of variability across time of day and between days, (ii) the coherence of spectral response across time of day, and (iii) if spectral channels (determined by sensor) affects the ability to resolve the dominant scale pattern. Semivariogram analysis was conducted for the region of interest (ROI) at 10, 100, 300 m spatial bins and at 14nm, MODIS and MERIS equivalent spectral bins. Semivariogram analyses have been used in the marine environment to document the spatiotemporal variability of several phenomena, including the determination of geographical patterns of chlorophyll variability for the global ocean¹⁰ and the cross-correlation of benthic and pelagic primary producer biomass along the California coast¹¹. For this study we selected a 5 x 5 km region in the northeast corner of Monterey Bay, centering at approximately 36.95 N and -121.93 W. In this initial study we used individual reflectance bands rather than derived products.

The statistics reported here are the lagged distance and semivariance values using “Queen’s move” pixel pairs (calculated with the software package, ENVI, ITT Visual Information Solutions, Boulder, CO). Queen’s move

calculates the squared difference over all pairs of pixels in the image in all eight directions. For a given wavelength, the nugget, sill, and range was determined by plotting the semivariance $\gamma(h)$, over distance between pixel pairs, h . For the commonly used spherical model of saturating semivariance, $\gamma(h)$, with increased distance, h , the equation for a theoretical semivariogram is as follows:

$$\gamma(h) = c_0 + c_1[(3h/2a) - 0.5(h/a)^3]$$

The non-zero intercept or nugget of the variogram, c_0 , determines the degree of unresolved variability; for sensor comparison it can represent the degree to which the particular pixel size captures the underlying phenomenon. The range, a , of a semivariogram determines how quickly the underlying variability reaches a global maximum, essentially the distance to which the structure of a variable is spatially dependent¹². Finally the sill, c_1 , determines the total variance resolved in the image or region of interest and the range beyond which the spatial structure of the data is not affected by the distance between sample units.

Equations based on real data may exhibit much more complex behavior than a theoretical spherical model with multiple nodes often apparent at distances less than saturation. For our experiment, we compared the nugget and range(s) to apparent node(s) across spatial and spectral bins sizes for data collected on two dates, 09/12/06 and 09/15/06. While these data are geolocated and radiometrically calibrated, they have yet to be atmospherically corrected; comparing absolute values (i.e. sills) would not be prudent. Therefore all variance data have been normalized to reflect percentage of maximal variances.

3 RESULTS

We first looked at temporal changes using the 10 m data (Fig. 5). On September 12th there is a dramatic change in the shape of the semivariogram over the course of an hour. Between 9 and 10 AM we see an increase in the intermediate scales of patchiness in the image. By the 10:06 AM image there are prominent nodes at 100, 200 and 450 m suggesting that these are dominate scales of patchiness. We relate this patchiness to the HAB b coming to the surface and forming patches on this scale which are clearly seen in the imagery (e.g. in Fig. 4). A strong wind event beginning on the evening of September 14th thoroughly mixed the water column and, by contrast, the semivariogram from September 15th does not show any dominate scale of patchiness.

Note that even for the 15th better than 90% of the variance is resolved in the 10 m data. This is not the case when the data are binned to 100 or 300 m (fig.6). One hundred meters does a reasonable job resolving 60 to 80% of the variance. However, when binned to 300 m we only resolve 60 to as little as 30% of the variance. In particular, only 30% of the variance is resolved at 300 m for the data from the 15th. This well mixed case is more typical for many coastal regions.

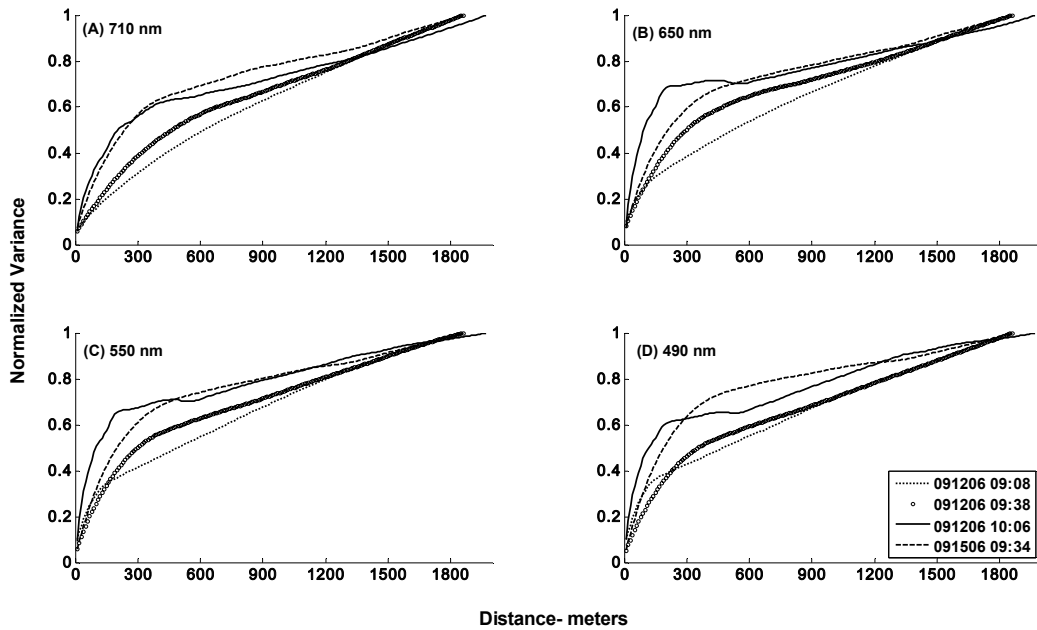


Fig. 5. Temporal changes in dominant spatial scales at 4 visible wavelengths using the 10 m GSD data. The first three variograms within each subplot were taken $\frac{1}{2}$ hour apart on the 12th of September, 2006: large HAB is present in this imagery. The final variogram is for an image at the same time of day, but three days later subsequent to a change in oceanic conditions that led to the temporary dissipation of the bloom.

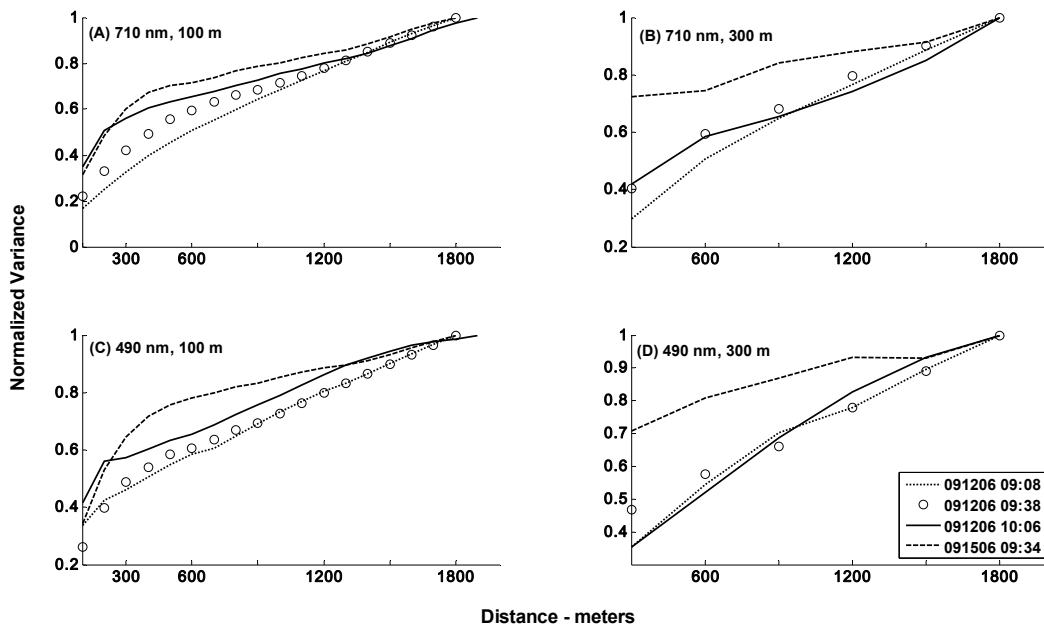


Fig. 6. The effect of pixel size on the ability to sample dominant spatial scales. The time frame of the four variograms in each subplot are as in Figure 1. The top subplots (A and B) represent the accumulating variance with increasing distances at 710 nm wavelength and pixel sizes of 100m and 300m respectively. The bottom two subplots (C and D) show the same information for 490 nm wavelength. Compare with the 10 m data in Fig. 1 a and d.

We also looked at the effect of spectral sampling on the ability to resolve the features in the image. We used the September 12th 10:06 AM data binned to 300 m to simulate a more typical satellite spatial resolution. The results show that for this particular case at 300 m there is no particular advantage to one or the other set of channels (Fig. 7). Note that the portion of unresolved variance increases sharply for wavelengths longer than 700 nm. This is likely because wavelengths longer than 700 nm do not penetrate more than a couple of meters into the water. At the time this image was collected only parts of the bloom have come to the surface resulting in small scale HAB patches near the surface visible in those wavelengths. At the shorter wavelengths these surface patches are seen as part of the larger submerged bloom feature which is better resolved in the 300 m data.

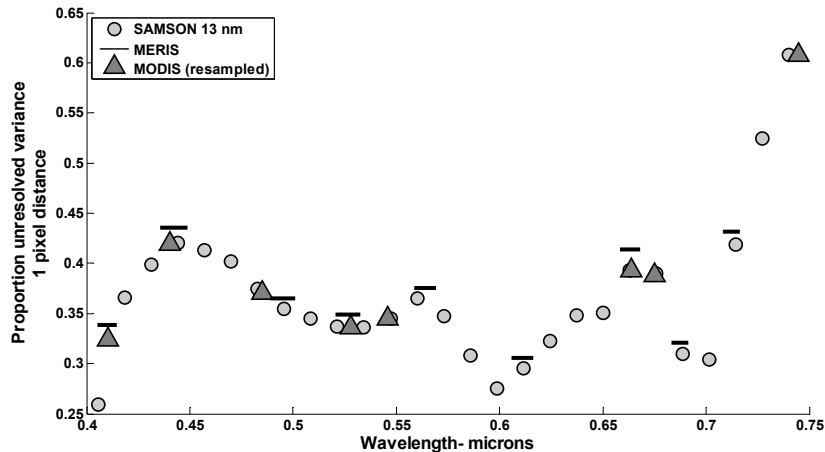


Fig. 7. Comparison of sensor performance at 300 meter pixel size. The proportion of unresolved variance is for each sensor is equivalent to the nugget in the variogram analyses. MODIS values for 300 m pixel sizes were derived by resampling original (3.5 nm) SAMSON data to MODIS wavelengths and response functions from ENVI. MERIS variance values were estimated using the SAMSON data and response function; the spectral ranges for individual MERIS bands are accurate.

We also examined the wavelength and pixel size dependence of the nugget effect for bloom and non bloom periods (fig. 8). A dinoflagellate bloom was apparent in images and the in situ data during the period including and prior to the 12th of September. There was a strong wind event on the evening of the 14th and by the 15th oceanographic conditions had changed leading to a temporary dissipation of the bloom. For both days the 10 m data essentially resolves all of the scales of variability at all wavelengths. On the 12th the 100 m and 300 m data work similarly for wavelengths shorter than 700 nm. For the wavelengths longer than 700 nm the 100 m data works better and the 300 m data is less effective at resolving the variability of the data. We attribute this difference to the surface patches formed by the HAB on the scales of 100 and 200 m (Fig 5a) that would have a strong signal at 710 nm and would be resolved in the 100 m data but would not be resolved in the 300 m data. As noted above 710 nm does not penetrate more than a couple of meters into the water. The patches seen at 710 nm appear smaller as they are the surface manifestation of the larger patches seen in the shorter more penetrating wavelengths. These large patches are better resolved in the 300 m data.

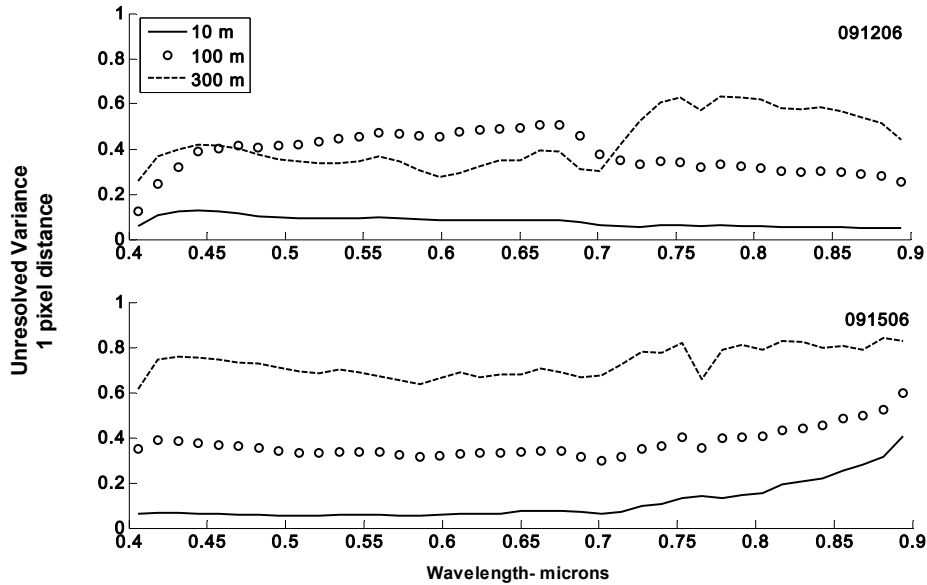


Fig. 8. Wavelength and pixel size dependence of “nugget effect” for bloom and non-bloom periods. The nugget effect is the unresolved variance at 1 interpixel distance. The same region was analyzed for dominant spatial scales with images taken on 091206 (10:06 am, top pane) and 091506 (09:38 am, bottom panel) with the SAMSON sensor.

4 DISCUSSION AND CONCLUSIONS

The results of this study are similar to an earlier study on the spatial requirements of a coastal ocean sensor inshore of 10 km⁵. In particular, turbid near shore waters require a GSD < 100 m to adequately resolve the spatial variance in the remotely sensed signal. That paper⁵ suggests that when you look at the whole spectrum, the scale of variability may actually get smaller for seemingly well mixed waters. Our results (Fig. 5) confirm that conclusion; the scale of variability is much smaller on September 15th when the water is well mixed.

That earlier study did not focus on the temporal changes in the reflectance signal, so was unable to comment on the possible cause in the spatial variance. Here, we hypothesize that the changing spatial variance and the requirements of the smaller GSD within the bloom was a function of the vertical migration of the dominant dinoflagellate in the bloom. This has significant ecological implications and is the first study that we know that suggests that remote sensing studies for species identification, biomass, and productivity could be significantly impacted by an under sampling of the spatial resolution of the bloom.

In contrast to the previous study⁵, we did not review the impacts on the combined spatial and spectral resolution simultaneously. That study suggested the use of the continuous high resolution reflectance spectral enabled the resolution of greater spatial variance in what was previously considered “homogeneous” waters. It is unclear if such a similar study would yield that same result.

The 709 nm channel was particularly helpful for identifying the HAB and demonstrates that utility/requirement of accurately resolving the Near-Infrared (NIR) reflectance in coastal waters. This channel is available on MERIS; however, none of the planned or on orbit U.S. satellite ocean color sensors carry this channel. Those sensors were developed for mapping the global ocean chlorophyll content and productivity of phytoplankton and they have worked extremely well for that application. The sensors rely on atmospheric correction schemes that (for the most part) assume a “black pixel”, or zero water-leaving radiance in the NIR. Clearly this is not the case in these images. This strongly demonstrates the need to resolve NIR water-leaving radiance should be a fundamental feature in the design of a CWIS to be used where HABs, river runoff and other bottom features yield significant radiance in the NIR. Our ability to

identify 709 nm as an indicator of this large plankton bloom demonstrates the utility of collecting hyperspectral data for these studies. This 709 channel or some other method of resolving NIR water-leaving radiance should be included in addition to any atmospheric correction channels for a CWIS.

Our analysis of three images from September 12th showed changes in patch size (Fig. 5) and visual inspection shows rapid movement of the HAB patches that is clearly resolved in the 10 m data. Further analysis is needed to identify the proper combination of spatial and temporal sampling to resolve critical coastal features. However, sampling on the order of once every 3 hours is minimal based on tidal currents and biological changes during the day. The frequent imagery from a CWIS will significantly improve our ability to monitor water quality, large oil spills, HABs and other features that are critical to the management of these areas. The imagery will also aid the development of ecosystem models for these important areas. Applications will include the management of marine sanctuaries, providing harmful algal bloom and other health warnings and improved management of fisheries using the Essential Fish Habitat approach for key commercial and sport fish stocks.

There is a growing concern about the health and future of the coastal ocean as expressed by the U.S. Commission on Ocean Policy in their report to Congress. In response Congress has already initiated an effort to establish an advanced Coastal Monitoring System and to improve coastal management practices to assure the future health of the coastal ocean for its many uses. The monitoring system includes the Integrated Ocean Observing System (IOOS) – which has an in-situ component, satellite remote sensing, and the development of advanced models of coastal ocean dynamics. A key part of that monitoring system will be a high frequency, high spatial and spectral resolution coastal waters imaging system (CWIS). That imager will provide the frequent imagery of the ocean surface that is needed to extend the in situ observations made by IOOS to the entire coastal zone. Additionally, the imager data will be essential for initiating and validating models of coastal ocean dynamics.

ACKNOWLEDGMENTS

We thank NOAA NESDIS for support for this effort. In particular we thank Stan Wilson and John Pereira for their support in establishing the COAST team and Paul Menzel for his support and help in making the COAST part of the GOES-R Risk Reduction Activities. We thank Mark Abbott COAST Team Leader and the rest of the COAST team for their insights and the use of their data from the COAST Monterey Bay Experiment to help us understand and interpret the remote sensing data.

REFERENCES

1. Esaias, W. E., Abbott, M. R., Barton, I., Brown, O. B., Campbell, J. W., Carder, K. L., Clark, D. K., Evans, R. H., Hoge, F. E., Gordon, H. R., Balch, W. M., Letelier, R., & Minnett, P. J., "An overview of MODIS capabilities for ocean science observations," *IEEE Transactions on Geoscience and Remote Sensing*, 36(4), pp. 1250-1265, 1998.
2. McClain, C. R., Feldman, G. C., and Hooker, S. B., "An overview of the SeaWiFS project and strategies for producing a climate research quality global ocean bio-optical time series," *Deep-Sea Res. II*, 51(1), pp. 5-42, 2004.
3. For information about VIIRS see http://www.ipo.noaa.gov/Technology/viirs_summary.html
4. For information about COAST go to <http://cioss.coas.oregonstate.edu/CIOSS/coast.html>
5. Bissett, W.P., Arnone, R., Davis, C.O., Dickey, T., Dye, D., Kohler, D.D.R. and Gould, R., "From meters to kilometers- a look at ocean color scales of variability, spatial coherence, and the need for fine scale remote sensing in coastal ocean optics", *Oceanography*, 17(2): 32-43, 2004.
6. Lee et al. 2007, Water and bottom properties of a coastal environment derived from Hyperion data measured from the EO-1 spacecraft platform, *J. Applied Remote. Sensing*, In Press.
7. Lee, Z. P., and Carder, K. L., "Effects of spectral-band number on retrievals of water column and bottom properties from ocean-color data", *Appl. Opt.*, 41, pp. 2191-2201, 2002.
8. MERIS information and data access at <http://envisat.esa.int/instruments/meris/>
9. Kohler, D.D.R., Bissett, W.P., Steward, R.G. and Davis, C.O., "A New Approach for the Radiometric Calibration of Spectral Imaging Systems", *Optics Express*, 12(11), 2004.

10. Doney SE, Glover DM, McCue SJ, and M Fuentes, "Mesoscale variability of Sea-viewing Wide Field-of-view Sensor (SeaWiFS) satellite ocean color: Global patterns and spatial scales", *Journal of Geophysical Research* 108: NO.C2, 3024, doi:10.1029/2001JC000843, 2003.
11. Broitman BR and BP Kinlan, "Spatial scales of benthic and pelagic producer biomass in a coastal upwelling ecosystem", *Marine Ecology Progress Series* 327:15-25, 2006.
12. Fortin M and Dale M, *Spatial analysis: A guide for ecologists*. Cambridge University Press. Cambridge UK, 2005.